Two-dimensional two-state lattice-gas model

O. M. Braun*
Institute of Physics, National Academy of Sciences of Ukraine, 03650 Kiev, Ukraine
and Department of Physics and Centre for Nonlinear Studies, Hong Kong Baptist University, Hong Kong

Bambi Hu
Department of Physics and Centre for Nonlinear Studies, Hong Kong Baptist University, Hong Kong
and Department of Physics, University of Houston, Houston, Texas 77204, USA
(Received 12 March 2004; revised manuscript received 7 October 2004; published 24 March 2005)

We propose a two-dimensional lattice-gas (2D LG) model where atoms may be in two different states: the immobile state, in which they jump as usual in the LG model, and the running state, in which the atoms always jump in the driving direction. The model demonstrates a typical behavior of "traffic-jam" models: the system splits into domains of immobile atoms (jams) and running atoms. We considered four variants of the 2D LG model, namely the multilane and truly 2D models, each with "passive" and "active" atomic jumps. The model has the steady state with a power law distribution of jam sizes characterized by a universal exponent $3/2$. The phase diagram of the model shows that the mobility of the 2D system is lower than the mobility of the 1D model due to the spreading of jams in the direction transverse to the driving direction.

DOI: 10.1103/PhysRevE.71.031111 PACS number(s): 05.40.−a, 45.70.Mg, 89.40.−a, 05.70.Ln

I. INTRODUCTION

Driven diffusive systems belong to the simplest models of nonequilibrium statistical mechanics. These systems are characterized by a locally conserved density, with a uniform external field setting up a steady mass current. The systems of this class have wide application in modeling charge and mass transport in solids and on crystal surfaces. Recently the driven diffusive models have been used in tribology, where the driving force emerges due to motion of one of two substrates, which are separated by a thin atomic layer.

One of the widely used models of this class is the generalized Frenkel-Kontorova (FK) model [1], where a one- or two-dimensional atomic system is placed into the external periodic potential, and the atomic current j in response to the driving force F is studied by solutions of Langevin motion equations. The simulations showed that when the force increases, the system goes from the low-mobility regime to the high-mobility state, where all atoms move with almost maximum velocity. In the underdamped case, when the external damping coefficient η in Langevin equations is lower than a characteristic frequency of atomic vibration at a minimum of the substrate potential, the model exhibits an interesting phenomenon of phase segregation: During the transition the atoms have a tendency to be organized in compact groups of two different types, one consisting only of slowly moving atoms which resemble traffic jams, and another of running atoms moving with the maximum velocity [2]. However, the FK model is too complicated to be studied in all details. For this reason it is important to develop a more simple model which will capture the most important features of the FK model. Although in this case we lose the possibility of exactly predicting the characteristics of a real physical object, a different sight on the problem could help us to understand the behavior of more realistic and complicated models.

Microscopically, the driven diffusive system may be modeled as a lattice gas (LG) where particles occupy the sites with at most one particle per site. The atoms jump stochastically to vacant nearest-neighbor sites, and the external field biases jumps in the positive x direction. Let us assume that an atom may jump to the right with probability α and to the left with probability $1-\alpha$, where $\frac{1}{2}<\alpha\leqslant 1$. Such variant of the LG model is known as the partially asymmetric exclusion model (ASEP) [3,4]. Driven lattice gases with hard-core repulsion traditionally are used to describe hopping diffusivity and conductivity in solids. The $\alpha=1$ variant of the ASEP model, called the totally asymmetric exclusion model, has been solved exactly [5]. Since the discovery of the exact solution, driven LG-type models have attracted much interest (e.g., see recent review papers [6,7] and references therein). Different variants of the model have been studied, in particular, in the context of modeling traffic flow [8–11]. In this context, the one-dimensional variant of the model was introduced in Refs. [12–14] (for a recent detailed discussion see Ref. [15]). Then the model was extended to multilane [16–20] and two-dimensional [21,22] variants.

A realistic continuous model such as the FK model mentioned above may be described by the LG model, if the thermal energy k_BT is much lower than the height of the substrate potential ε, and the atoms interact via the hard-core potential. In this case the probability of an atomic jump to the right at a small applied external force F is $\alpha\approx(1+e^{-aF/T})^{-1}$, where a is the lattice spacing, so that the parameter α in the LG model plays the role of the driving force.

The underdamped FK model has, however, one more aspect connected with the existence of external damping in Langevin equations. When the damping coefficient η is large, the atom after the jump stops in the new potential well. But if η is small, there exists a threshold force

*Electronic address: obraun@iop.kiev.ua

F_b ($F_b \approx \eta\sqrt{m\varepsilon}$, m being the atomic mass) such that at $F > F_b$ the atom after the jump does not stop but continues to move until it meets a stopper, e.g., a thermalized atom in front of itself. To incorporate this feature into the lattice-gas model, one may assume that an atom may be in two different states, in the "thermalized" state, in which it jumps as usual in the LG model, and in the "running" state, in which the atom always jumps to the right provided the right-hand site is empty. Thus our model incorporates the features of both partially and totally asymmetric models. Models with multiple states belong to cellular automata type models which are widely used, in particular, in simulation of highway traffic [8–22].

In our previous paper [2] we have introduced and studied a one-dimensional variant of the two-state lattice-gas model. Because it will be used throughout the present work, let us recall briefly the model and the main results. We considered a one-dimensional (1D) lattice of length M with periodic boundary conditions. Let N be the total number of atoms so that the dimensionless concentration is $\theta = N/M$. Then, let us assume that an atom may be in *two different states:* the "immobile" state, in which it jumps as usual in the LG model, and the "running" state, in which the atom always jumps to the right provided the right-hand site is empty. The atom can change its state from the immobile state to the running state and vice versa: the immobile atom is in the running state after a jump to the right, and the running atom becomes immobile after a "collision" with an immobile atom. The system evolves in time according to the random-sequential dynamics (the parallel dynamics leads to similar results [23]), i.e., atoms jump independently and randomly according to the following rules: (i) At each time step $t \to t+1$, one chooses a site i at random; (ii) If this site is occupied by an immobile atom, it jumps to the site $i+1$ (if this site is empty) with probability α or it jumps to the site $i-1$ (if the left-hand site is empty) with probability $1-\alpha$ as in the partially asymmetric exclusion model. After the jump to the left the atom remains in the immobile state, while *after the jump to the right the atom is in the running state*; (iii) If the atom in the chosen site i is in the running state, it jumps to the right provided the right-hand site is empty, and remains in the running state. Otherwise, if the site $i+1$ is not empty, the atom at the site i remains in the running state if the right-hand site is occupied by the running atom, or *becomes immobile if the site* $i+1$ *is occupied by the immobile atom*.

This simple model demonstrates a typical behavior of traffic-jam models, where the atoms behave similarly to vehicles in a one-lane road. At the same time, this model admits an analytical description. From the very beginning the system splits into compact domains of immobile and running atoms. The immobile domains (jams) are characterized by the local atomic concentration $\theta_s = 1$. The jams are separated by running domains characterized by a local concentration $\theta_r < \theta$. To characterize the system state, we introduce the dimensionless "mobility" B as the ratio of the number of running atoms N_r to the total number of atoms N, $B = N_r/N$. To calculate B analytically, one may suppose that there is only a single jam of length N_s in the chain. Because the local concentration in the jam is $\theta_s = 1$, we can apply the following simple arithmetic:

$$N_s + N_r = N, \quad N_s + M_r = M, \tag{1}$$

where M_r is the length of the running domain (RD). Taking into account that $N_r = M_r\theta_r$ and $N = M\theta$, we obtain $N_s = M(\theta - \theta_r)/(1-\theta_r)$, so that the mobility is equal to

$$B = \frac{\theta_r(1-\theta)}{(1-\theta_r)\theta}. \tag{2}$$

Evidently, Eq. (2) should be valid also for the steady state with any number of jams provided θ_r corresponds to the mean atomic concentration in the RD's.

According to the rules accepted above, the left-most site of any RD is always empty. Therefore the running domain grows from its left-hand side at the rate α due to an injection of new atoms from the left-hand-side neighboring jam. At the right-hand side of the RD, the atom which occupies the right-most site of the RD leaves the RD and joins itself to the neighboring right-hand-side jam. Thus the RD shortens from the right-hand side at the rate p_r, where p_r is the probability that the right-most site of the RD is occupied. Clearly, in the steady state $p_r = \alpha$. Neglecting by a possible deviation of the RD concentration at its right-hand side from the mean value θ_r, we may take approximately

$$p_r \approx \theta_r, \tag{3}$$

and finally we come to the expression

$$B \approx \frac{\alpha(1-\theta)}{(1-\alpha)\theta}, \quad \alpha < \theta. \tag{4}$$

For $\alpha > \theta$ the jams disappear at all, and $B = 1$ in the steady state. The expression (4) is in excellent agreement with the results of numerical simulation [2].

Another interesting feature of this model is that at $\alpha < \theta$ the infinite system has no steady state at all. Indeed, a jam of length s loses atoms from its right-hand side at the rate α, and it receives new atoms to the left-hand side at the rate p_r. These two rates are equal to each other in the steady state, so on average $\langle \dot{s}(t) \rangle = 0$. However, due to the randomness of joining and losing events, the value $s(t)$ should exhibit random walks, i.e., at long times $s(t)$ must behave according to the diffusional equation

$$\langle [s(t) - s(t')]^2 \rangle \doteq 2\alpha|t - t'|. \tag{5}$$

Thus when a jam reaches the size $s = 0$, it disappears forever, while the evolution of $s(t)$ to higher values is not restricted in the infinite system. The distribution of jam sizes $P(s)$ continuously changes with time shifting to larger and larger values (see simulation results in Ref. [2]) and approaches the Gaussian distribution $P(s,t) \propto \exp(-s^2/4\alpha t)$ (see the Appendix). Therefore instead of the name "steady state" it is more reasonable to use the name "coarsening state." However, the mobility of the coarsening state does not change with time because B is determined by the system parameters only according to Eq. (4).

The model described above is similar to the simplest variant of the Nagel-Schreckenberg (NS) "minimal" model of real traffic [12–14] with a maximum velocity of 1. The present model differs from the NS model in two aspects:

first, we use sequential dynamics contrary to the "parallel update" of the NS model; and second, the low-velocity state of our model corresponds to thermalized atoms while in the NS case it corresponds to immobile cars (in cellular automata traffic-jam models the immobile cars typically cannot move backward, while in the LG model the backward jumps are allowed). Both these features are natural for the system of atoms in contact with a thermal bath. If we introduce the atomic flux as $j=\theta v$, where v is the average velocity of the atoms (this is the standard expression for the flux in LG-type models), then the main issue of the traffic theory, the fundamental diagram (flux vs density) takes the trivial form $j=\theta(1-\theta)$. However, in the Frenkel-Kontorova type model, where all atoms in the running domain move simultaneously, it is more natural to define the "flux" as $j=\theta B$, where the "mobility" B was introduced above. For this definition of j, the fundamental diagram takes the triangular shape, $j=\theta$ for $\theta<\alpha$ and $j=(1-\theta)\alpha/(1-\alpha)$ for $\theta>\alpha$, which is similar to that of real traffic [8–14].

The aim of the present paper is to extend the driven LG model to two dimensions. Our main question of interest is the following: Is the mobility of a 2D model higher or less than that of the 1D model. Indeed, in the 1D model a single jam blocks the motion along the chain. Thus, in a 2D model, where an atom can pass around a jam, one could expect a higher mobility than in the 1D model. Surprisingly, the answer is just the opposite: the mobility of 2D models in most cases is lower than that of the 1D model with the same parameters! Another drastic difference compared to the 1D case is that the 2D model does have a true steady state which is characterized by a power law distribution of jam sizes with a universal exponent 3/2. Moreover, these features of the 2D two-state LG model are generic: We considered four different variants of the model, such as "multilane" and "truly 2D" models, as well as the models with "passive" and "active" jumps, and checked that all variants of the model lead to the same qualitative results.

The paper is organized as follows. Four versions of the 2D generalization of the model, namely the multilane and truly 2D models with passive and active jumps are introduced in Sec. II. Simulation results together with some analytical ones are presented in Sec. III. In Sec. IV we present the attempts to explain the simulation results qualitatively. Finally, Sec. V concludes the paper.

II. MODEL

We consider a generic example of a two-dimensional model, namely the most isotropic lattice with triangular symmetry (see Fig. 1). Every site may be either empty or occupied by an atom. Every atom may be in one of two states: the "immobile" state or the "running" state. The immobile atom may jump to one of six neighboring sites, provided this site is empty. Three of these sites, the forward (f), forward up (fu), and forward down (fd), are in the direction of the driving. We assume, analogous to the 1D model described in the Introduction, that after the jump to one of these three sites, the atom is in the running state.

Jump probabilities. Let α_f, α_{fu}, α_{fd}, α_b, α_{bu}, and α_{bd} be the probability for an immobile atom to jump to the empty right-hand site, right-up site, right-down site, left-hand site, left-up site, and left-down site, respectively, as shown in Fig. 1. An asymmetry in jump rates emerges due to the external driving force F, because the rate of an activated jump is proportional to $\exp(-\varepsilon'/T)$ and the barrier is changed due to the force as $\varepsilon'=\varepsilon-a'F$, where $a'=\pm a$ for the forward/backward jumps and $a'=\pm a/2$ for the $fu/fd/bu/bd$ jumps. Therefore we may assume that $\alpha_f=\alpha_0 c^2$, $\alpha_{fu}=\alpha_{fd}=\alpha_0 c$, $\alpha_b=\alpha_0/c^2$, and $\alpha_{bu}=\alpha_{bd}=\alpha_0/c$, where $c\sim\exp(aF/2T)$. Then, taking into account the normalization condition $\alpha_f+\alpha_{fu}+\alpha_{fd}+\alpha_b+\alpha_{bu}+\alpha_{bd}=1$ and defining the total probability of the jump in the driving direction as $\alpha=\alpha_f+\alpha_{fu}+\alpha_{fd}$, we can find the parameters α_0 and c and express all jump rates as functions of a single parameter α as shown in Fig. 2.

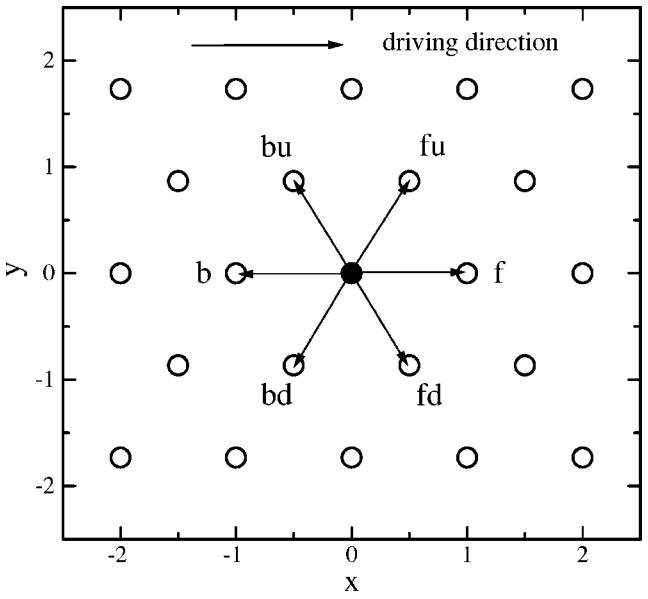

FIG. 1. Triangular lattice.

In analogy to the 1D model described in the Introduction, let us introduce the following updating rules for the 2D model: (i) At each time step $t\to t+1$ we choose an atom at random; (ii) if this atom is in an immobile state, it jumps to one of six neighboring sites with a corresponding probability provided the chosen site is empty. After the jump to one of three backward directions (in the b, bu, or bd direction) the atom remains in the immobile state, while after the jump to the direction of driving (the f, fu, or fd direction) the atom is in the running state; (iii) if the chosen atom is in the running state, its behavior is different for the following four variants of the model.

Multilane and truly 2D models. The difference between the multilane and truly 2D models is that in the multilane model, similar to the 1D model, the running atom jumps to the right (in the f direction of Fig. 1) provided the site ahead of the running atom is empty, while in the truly 2D model the running atom remembers the direction of the previous jump (an analog of inertia effect in Newtonian dynamics) and continues to jump in the same direction (i.e., in the f, fu, or fd direction). After the jump, the atom remains in the running state. If the site, to which the running atom has to jump, is

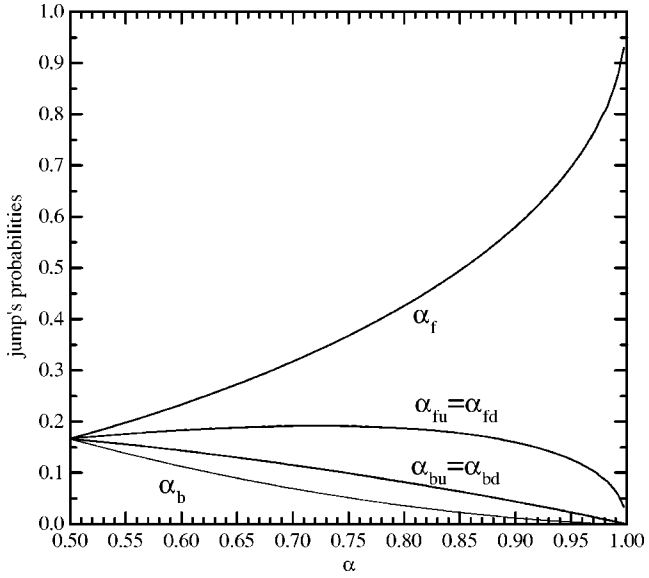

FIG. 2. Probabilities of the jump to the right α_f, right-up/down $\alpha_{fu}=\alpha_{fd}$, to the left α_b, and left-up/down $\alpha_{bu}=\alpha_{bd}$ as functions of α.

occupied by a running atom, both atoms remain in the running state (in the truly 2D model we assume in addition that these two running atoms exchange by their jumping directions, similar to momentum exchange in Newtonian dynamics). However, if the site, to which the running atom has to jump, is occupied by an immobile atom, the behavior is different for two more variants of the model to be described below.

Passive and active jumps. In the model with passive jumps, the running atom becomes immobile if the site, to which the running atom has to jump, is occupied by an immobile atom analogous to the 1D model. On the other hand, in the model with active jumps the running atom becomes immobile only if all three sites (*f*, *fu*, and *fd* in Fig. 1) are occupied by immobile atoms. If one of these sites is empty, the running atom jumps to this site (in the case of two empty sites the jumping site is chosen randomly).

Finally, we use periodic boundary conditions in both directions.

III. RESULTS

A. Steady-state and jam sizes distribution

If one starts with a random initial configuration, the system quickly reaches a steady state with a constant mobility B as shown in Fig. 3 (notice that B is lower than the mobility of the 1D model for the same values of α and θ, and that B grows as the lattice size increases in the vertical direction, reaching a plateau at $M_y \gtrsim 32$). Contrary to the one-dimensional model, however, now the system reaches a truly steady state, the distribution of immobile island sizes $P(s)$ does not change with time as demonstrated in Fig. 4.

Moreover, the distribution $P(s)$ is not Gaussian as in the 1D model, but follows the power law: for *all* variants of the 2D model as well as for *all* checked sets of the parameters α

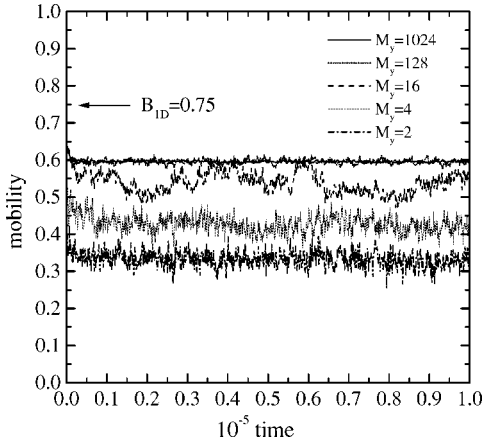

FIG. 3. The mobility B as a function of time for the multilane model with active jumps for different lattice sizes M_y in the vertical direction. The parameters are $\alpha=0.75$, $\theta=0.8$, and $M_x=1024$.

and θ the distribution $P(s)$ may be well fitted by the power law $P(s) \propto s^{-3/2}$. A typical example is presented in Fig. 5 (see also Ref. [26]).

The power-law distribution may be explained analytically if we consider the statistics of coalescence and splitting of immobile islands. Let $P_t(s)$ be the distribution of immobile islands at time moment t, $R(k+s,k)$ be the rate (per one time unit) of splitting of the island of size $k+s$ into two smaller islands k and s, and $T(k+s,k)$ be the rate of coalescence of

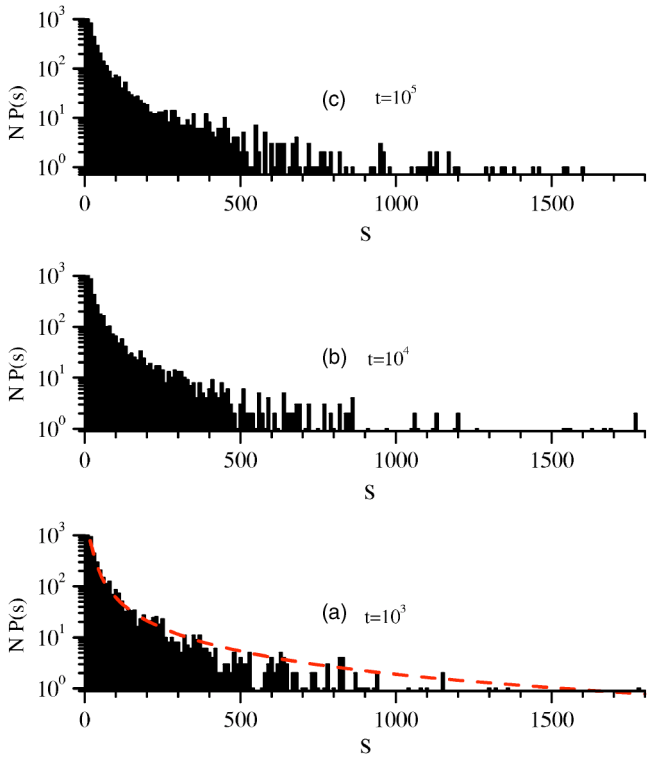

FIG. 4. (Color online) Histogram of size distribution of immobile islands for the multilane model with active jumps at different times: (a) $t=10^3$, (b) $t=10^4$, and (c) $t=10^5$ [dashed red curve shows the fit $P(s)=6\times10^4\ s^{-3/2}$]. The parameters are $\alpha=0.75$, $\theta=0.8$, and $M_x=M_y=1024$.

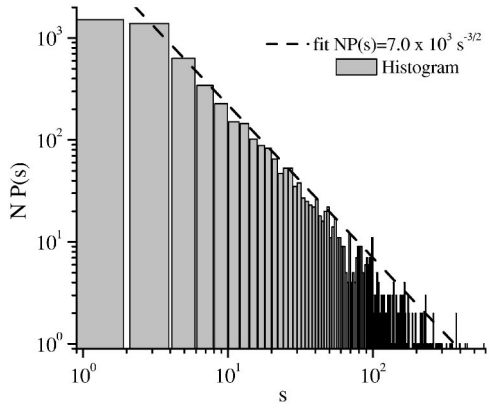

FIG. 5. Histogram $P(s)$ for the truly 2D model with active jumps. The parameters are $\alpha=0.95$, $\theta=0.8$, $M_x=M_y=512$, $t=10^3$, $B\approx 0.64$.

two islands k and s into one island of size $k+s$. Clearly, $R(k+s,s)=R(k+s,k)$ and $T(k+s,s)=T(k+s,k)$.

Now we can write the master equation as follows:

$$\Delta P_{t+1}(s) \equiv P_{t+1}(s) - P_t(s) = \sum_{k=1}^{\infty} P_t(k+s)R(k+s,s) - P_t(s)\sum_{k=1}^{s-1} R(s,k) + \sum_{k=1}^{s-1} T(s,k)P_t(k)P_t(s-k) - P_t(s)\sum_{k=1}^{\infty} T(s+k,k)P_t(k). \quad (6)$$

The first term in the right-hand side of Eq. (6) describes the increase of the number of islands of size s due to splitting of higher-size islands, the second term describes the decrease of $P_t(s)$ due to splitting of the s island in two smaller parts, the third term describes the growing of the number of s islands due to coalescence of two smaller islands k and $s-k$, and the last term describes the decrease of the number of s islands due to their coalescence with other islands.

The steady state must satisfy the equation $\Delta P_t(s)=0$. It is natural to suppose that the rate of coalescence does not depend on the sizes of colliding islands, $T(s,k)=T_0$ for all s and k. The splitting rate $R(s,k)$, however, may depend on the shape of the splitting island and thus it will depend on both arguments s and k. To simplify consideration, let us assume that $R(s,k)$ depends on the size of the island only, $R(s,k) \approx R(s)$. In this case $R(s)$ should behave as $R(s)\propto(s-1)^{-1}$ for $s\gg 1$. Indeed, substituting $T(s,k)=T_0$ and $R(s,k)=R(s)$ into Eq. (6) for the steady state, we obtain

$$P(s)[(s-1)R(s)+T_0] = \sum_{k=s+1}^{\infty} P(k)R(k) + T_0\sum_{k=1}^{s-1} P(k)P(s-k). \quad (7)$$

Equation (7) can be rewritten in the form

$$R(s) = [T_0 a(s) + b(s)]/(s-1), \quad (8)$$

where

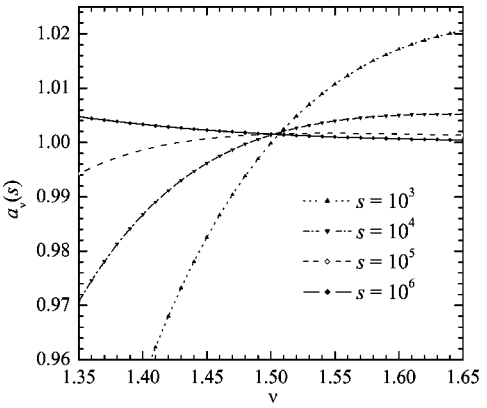

FIG. 6. $a_\nu(s)$ as a function of ν for different s.

$$a(s) = -1 + \sum_{k=1}^{s-1} P(k)P(s-k)/P(s) \quad (9)$$

and

$$b(s) = \sum_{k=s+1}^{\infty} R(k)P(k)/P(s). \quad (10)$$

Therefore the splitting rate has to have the form

$$R(s) = R_0/(s-1) \text{ for } s \gg 1 \quad (11)$$

provided the function $a(s)$ has a finite value at the $s\to\infty$ limit, $0<\lim_{s\to\infty} a(s)<\infty$. Then, substituting Eq. (11) into Eq. (7), one can see that the latter has a solution in the $s\gg 1$ limit only for the power-law distribution of island sizes,

$$P(s) = \zeta^{-1}(\nu)s^{-\nu}, \quad (12)$$

where $\zeta(\nu)$ is the Riemann zeta function.

The substitution of the distribution (12) into Eq. (9) yields

$$a_\nu(s) = -1 + \zeta^{-1}(\nu)s^{\nu}\sum_{k=1}^{s-1} k^{-\nu}(s-k)^{-\nu}. \quad (13)$$

Numerical investigation of this function suggests that it has a nonzero limit at $s\to\infty$ for one value of the exponent ν only, namely $\nu\approx 3/2$, as demonstrated in Fig. 6. The same result follows from analytical consideration of the function (13) with the help of Maple software, which shows that such a limit exists for $\nu=3/2$ only, and $a_{3/2}(\infty)=1$. Taking also into account the simulation results such as presented in Fig. 5, we conclude that the power-law distribution (12) with the exponent $\nu=3/2$ is the truly steady-state solution of the model under study.

Finally, the self-consistent solution of the steady-state distribution is achieved with the parameters $R_0=CT_0$, where $C\approx 3$ is a numerical constant.

B. Shape of jams

Qualitatively, the dependence of the mobility B on the model parameters α and θ is similar to that of the 1D model: B grows when α increases or when θ decreases and it is

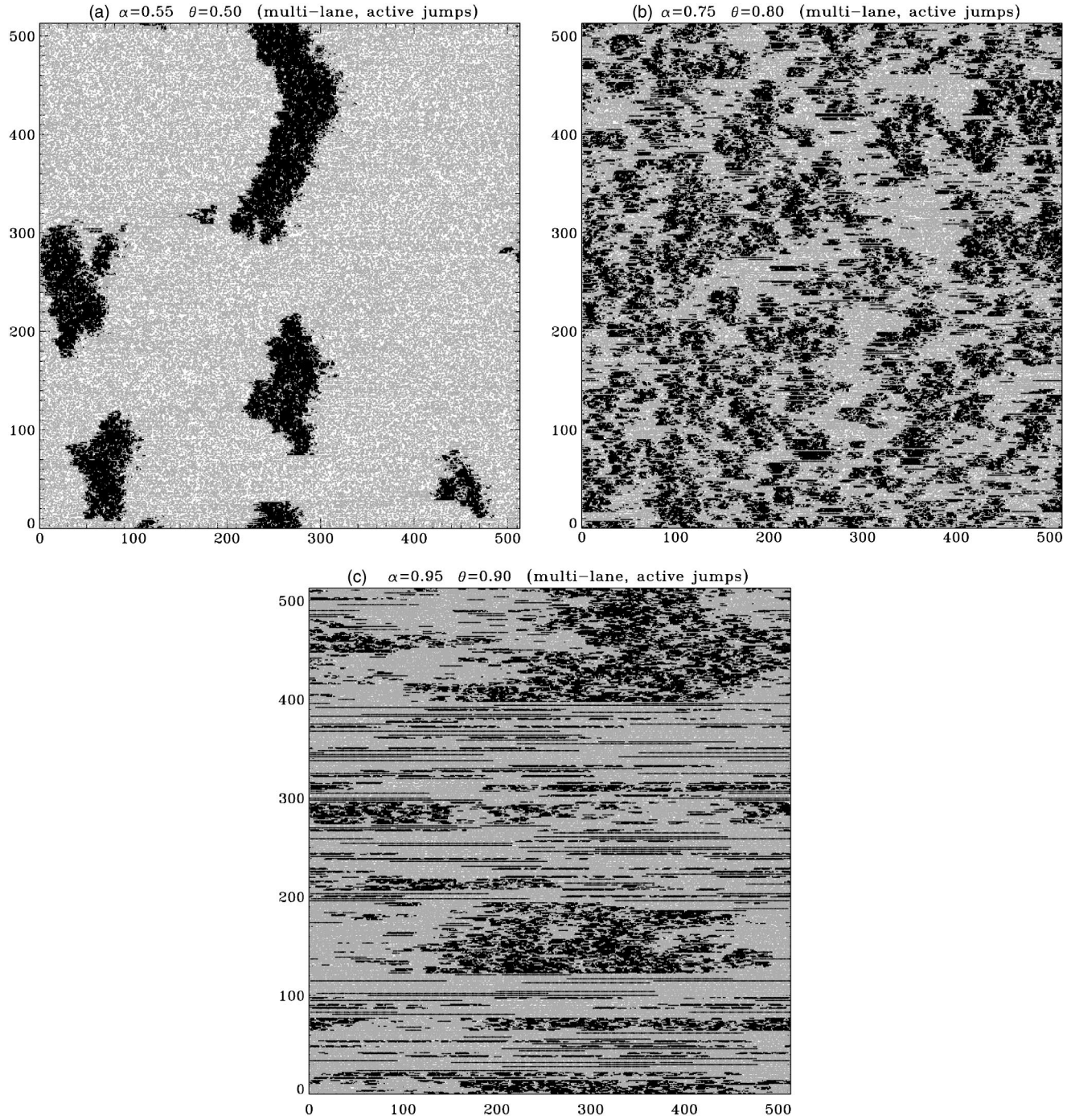

FIG. 7. Shape of jams. Snapshot configurations at $t=10^5$ of the multilane model with active jumps (lattice 512×512) for different model parameters: (a) $\alpha=0.55$, $\theta=0.5$, $B\approx0.8$; (b) $\alpha=0.75$, $\theta=0.8$, $B\approx0.6$; and (c) $\alpha=0.95$, $\theta=0.9$, $B\approx0.7$. Immobile atoms are in black and running atoms in grey.

determined by θ_r through the expression (2), although the simple expressions (3) and (4) are not valid for the 2D model. At a small enough concentration $\theta<\theta_c$, where the critical value θ_c depends on α as well as on the variant of the model, all atoms are in the running state and $B=1$. When $\theta>\theta_c$ and the concentration increases, more and more immobile islands emerge in the sea of running atoms. As far as $B>0.5$, these islands are isolated, and their shape depends on the "forcing" α: the immobile islands are elongated in the y direction at small α as shown in Fig. 7(a), approximately circular at intermediate values of α [see Fig. 7(b)], and elongated in the x direction (along the driving) at large α [Fig. 7(c)].

An average size of jams depends on the system size because $\langle s\rangle\sim\int dssP(s)\propto s^{1/2}|_N\propto(M_xM_y)^{1/2}$. Clearly, the maximum size s_m of the immobile island is determined by the system size too. Indeed, in a finite system the total number of immobile atoms may be written as $N_s\propto P(1)+2P(2)$

$+3P(3)+\cdots+s_mP(s_m)$. If we suppose that there is only one island with the maximum size, this relationship may be rewritten as $N_s=s_m^{1/2}\Sigma_{s=1}^{s_m}s^{-1/2}$, and the latter yields $s_m\approx 0.5N_s$ for $N_s\gg 1$.

As θ increases, the concentration of immobile islands grows, and at some critical concentration $\theta_p(\alpha)$, which corresponds to the percolation threshold for the given variant of the model, the jams begin to overlap. After that, the immobile atoms are arranged either into y-oriented strips [for smaller values of α, see Figs. 8(a) and 9(a)] or, at larger values of α, they create a two-dimensional net as shown in Figs. 8(b) and 9(b).

C. Comparison of different variants of the model

Passive and active jumps: The comparison of the mobility of models with passive and active jumps is presented in Fig. 10. A trivial result is that active jumps lead to a higher mobility. One can see also that the effect is stronger for the truly 2D model.

Multilane and truly 2D models: Let us also compare the multilane and truly 2D models (see Fig. 10). A surprising result is that for all cases, except the one with active jumps at low driving $\alpha=0.55$, the mobility of the truly 2D model is smaller than that of the multilane model.

2D and 1D models: Finally, let us compare 2D variants of the traffic-jam model with the simple 1D model described in the Introduction. As seen from Fig. 11, the mobility of the 1D model is higher than that of 2D variants of the model for almost all model parameters.

Figure 12 presents the phase diagram of four variants of the model. The curves separate the running ($B=1$) and jamming ($B<1$) states.

IV. DISCUSSION

To explain qualitatively the variation of $B(\theta)$ for different variants of the 2D model, let us look at some typical configurations below the percolation threshold (when $B>0.5$, see Fig. 13) and above the percolation (when $B<0.5$, see Fig. 14). These configurations were calculated for the lattice 512×512 and $t=10^5$; the figures show a zoomed region of size 96×96 extracted from a larger configuration.

From a general point of view, the mobility B of the 2D model should be higher than that of the 1D model because the atoms that collide with a jam may not stop but instead go around the jam. At the same time, however, B may be strongly decreased compared with the 1D model due to the spreading of jams in the y direction. The mobility B can be expressed through the concentration of the running atoms θ_r with the help of Eq. (2). Using the simulation data, we can plot θ_r as a function of θ for different values of the parameter α (see Fig. 15). In what follows we will try to give a crude qualitative description of the $\theta_r(\alpha,\theta)$ dependence. We will do this separately for the case of high mobility when the immobile islands do not overlap, and the case of low mobility, i.e., above the percolation of the islands.

The case of high mobility ($B>0.5$). In this simpler case the immobile islands are separated from each other as can be seen from Fig. 13. Let $\alpha(s)$ be an average rate of atomic jumps from the right-hand-side boundary of the immobile island of size s, provided the corresponding site is not occupied by a running atom. We have $\alpha(s)\approx\alpha\equiv\alpha_f+\alpha_{fu}+\alpha_{fd}$ for $s\sim 1$ as well as for immobile islands strongly elongated in the x direction, and $\alpha(s)\approx\alpha_f+0.5(\alpha_{fu}+\alpha_{fd})$ for $s\gg 1$ or for islands strongly elongated in the y direction (e.g., for the

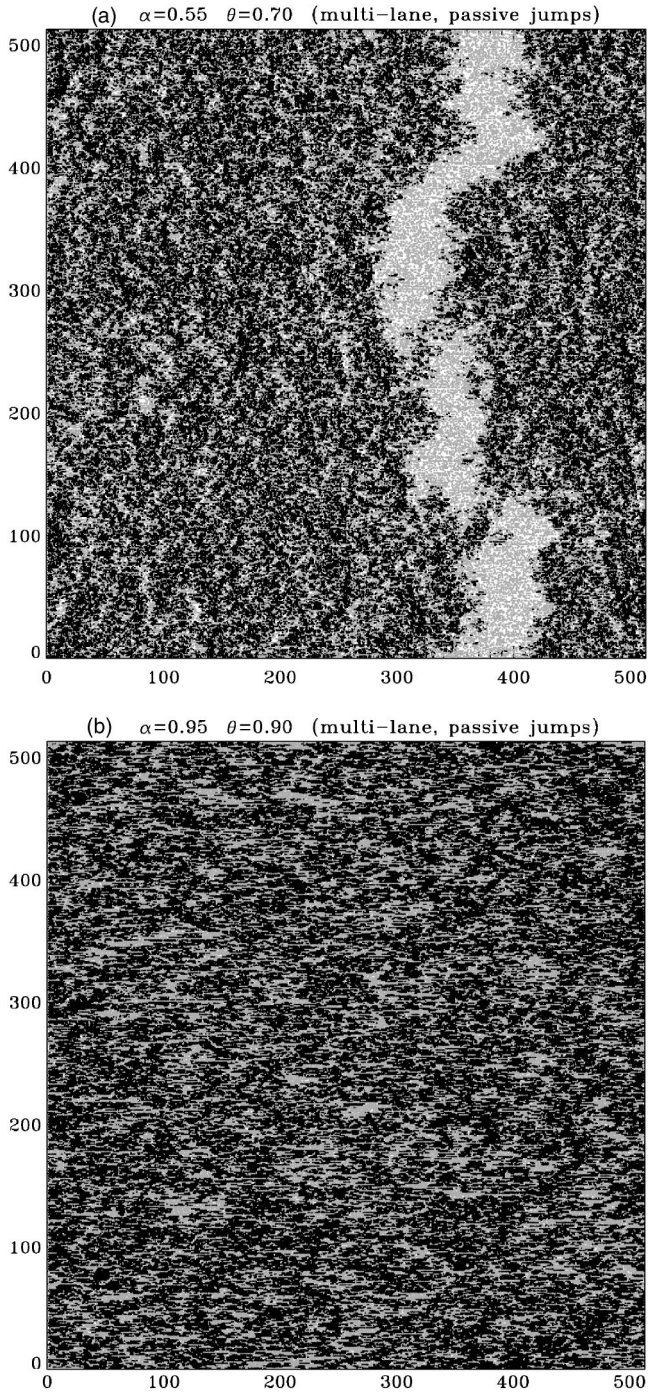

FIG. 8. Snapshot configurations at $t=10^5$ of the multilane model with passive jumps for: (a) $\alpha=0.55$, $\theta=0.7$, $B\approx 0.37$, and (b) $\alpha=0.95$, $\theta=0.9$, $B\approx 0.35$. Immobile atoms are in black and running atoms in grey.

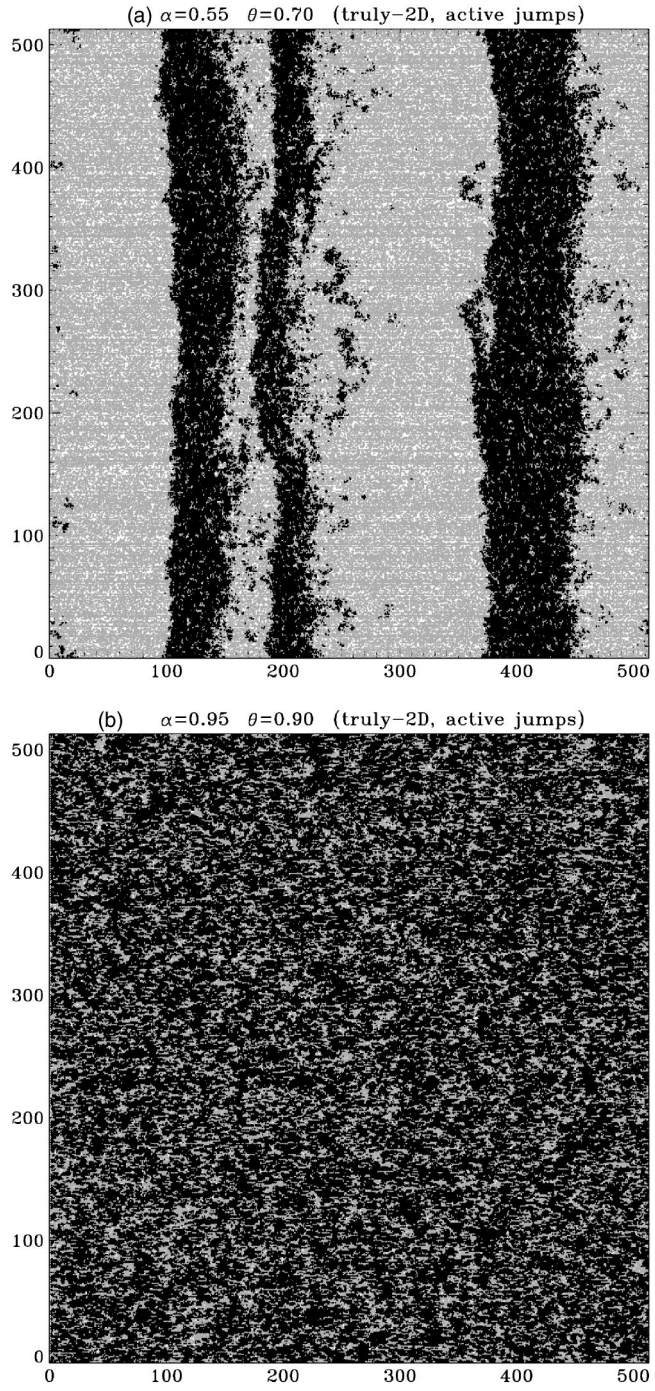

FIG. 9. Snapshot configurations at $t=10^5$ of the truly 2D model with active jumps for: (a) $\alpha=0.55$, $\theta=0.7$, $B\approx 0.57$, and (b) $\alpha=0.95$, $\theta=0.9$, $B\approx 0.26$. Immobile atoms are in black and running atoms in grey.

case of a flat vertical boundary). The jump's rate averaged over the whole system may be defined as

$$\overline{\alpha}=\frac{P(1)\alpha(1)+\cdots+P(s_m)\alpha(s_m)}{P(1)+\cdots+P(s_m)}. \tag{14}$$

If we assume that the dependence $\alpha(s)$ may be described by the following interpolation formula:

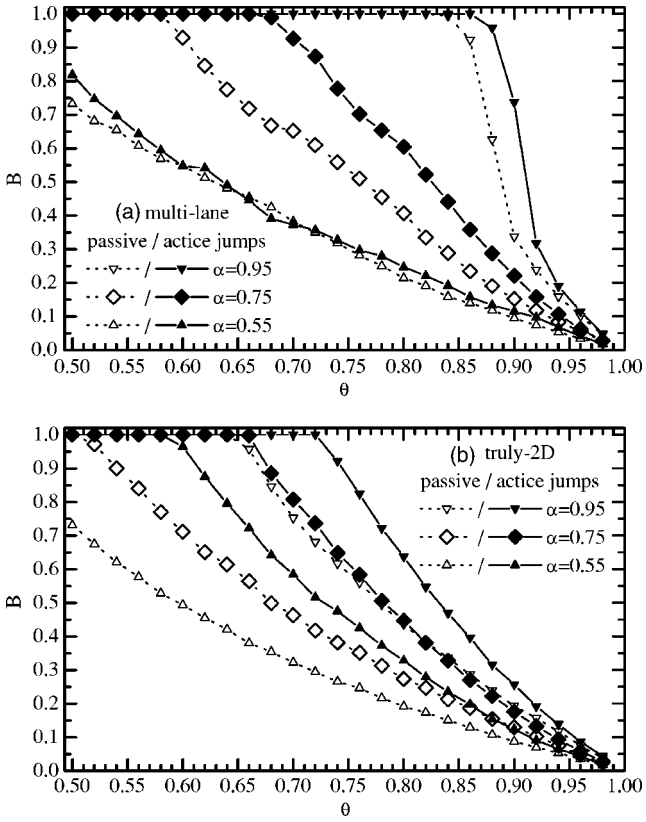

FIG. 10. The mobility B versus the concentration θ for (a) multilane and (b) truly 2D models with passive jumps (dotted curves and open symbols) and active jumps (solid curves and symbols) for three values of the driving: $\alpha=0.55$ (up triangles), $\alpha=0.75$ (diamonds), and $\alpha=0.95$ (down triangles). Lattice size is 256×256, and averaging is over 10^4 MC steps per atom.

$$\alpha(s)=\alpha_f+0.5(\alpha_{fu}+\alpha_{fd})(1+s^{-\xi}),$$

where $0<\xi<\infty$ is a parameter, then $\overline{\alpha}=\alpha_f+[1+G(\xi)]\alpha_{fu}$, where $G(0)=1$, $G(1)=\zeta(5/2)/\zeta(3/2)\approx 0.514$, $G(2)=\zeta(7/2)/\zeta(3/2)\approx 0.431$, and $G(\infty)=1/\zeta(3/2)\approx 0.383$. Because these values do not depend essentially on the exponent ξ provided $\xi\geqslant 1$, we may take in what follows $\xi=2$ so that $\overline{\alpha}\approx\alpha_f+1.43\alpha_{fu}$.

In the 1D model described in the Introduction, the site ahead of the right-most atom of the jam was always empty, thus the jam is shortened from its right-hand side at the rate $q=\alpha$. This is not true anymore for the 2D model: as can be seen from Fig. 13, some sites ahead of the right-hand boundary of the 2D jams are occupied by running atoms with some nonzero probability θ'. Thus in the 2D model the jam will shorten from its right-hand boundary at the rate $q=\overline{\alpha}(1-\theta')$. Then, let l be a linear size of the immobile island in the y direction from its left-hand side (i.e., l is the average jam's "cross section" for the incoming running atoms), and l_f be the (fractal) length of the island boundary from its right-hand side. The rate of growth of the jam (from its left-hand-side boundary) is $\theta_r l$ while the rate of its decrease (from the right-hand-side boundary) is ql_f. In the steady state these two rates must be equal to each other on the average. Thus we come to

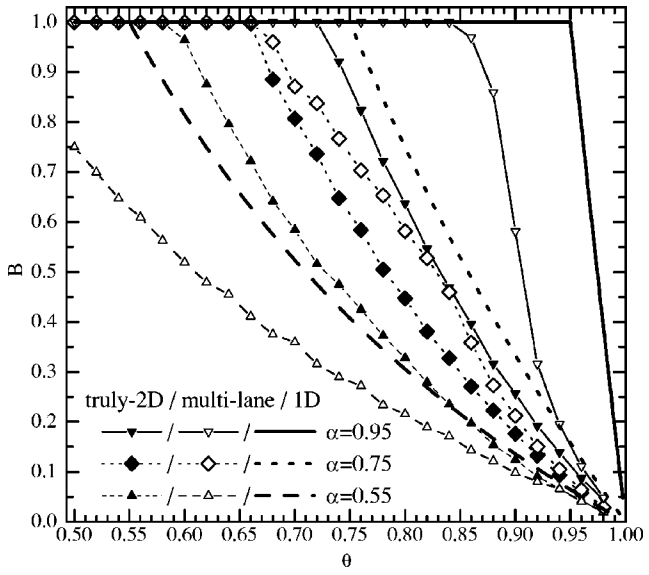

FIG. 11. $B(\theta)$ for the multilane model (open symbols) and truly 2D model (solid symbols) (both models with active jumps) compared with the mobility of the 1D model for three values of driving: $\alpha=0.55$ (up triangles and dash curves), $\alpha=0.75$ (diamonds and dotted curves), and $\alpha=0.95$ (down triangles and solid curves). Lattice size is 256×256, and averaging is over 10^4 MC steps per atom.

the expression $\theta_r=\overline{\alpha}Q$, where $Q=(1-\theta')\langle l_f\rangle/\langle l\rangle$.

The value $\overline{\alpha}$ is shown in Fig. 15 by a dashed line. One can see that the approach presented above describes the simulation data for the multilane model with passive jumps at $\theta \gtrsim \theta_c$ if we take $Q\approx0.91-0.96$. Although this value is reasonable, unfortunately we were not able to find Q analytically. A lower mobility of the truly 2D model compared with the multilane one could be explained by a lower value of the ratio $\langle l_f\rangle/\langle l\rangle$. On the other hand, a higher mobility of the models with active jumps compared with those with passive jumps can be easily explained by the decrease of the cross section: In the model with active jumps the parameter Q should be defined as $Q=(1-\theta')\langle l_f\rangle/\langle l-2\rangle$ because the "extreme" up/down running atoms colliding with the jam can now overcome it. As can be seen from Fig. 16, in the models with active jumps the concentration of running atoms increases by 1.1–1.3 times.

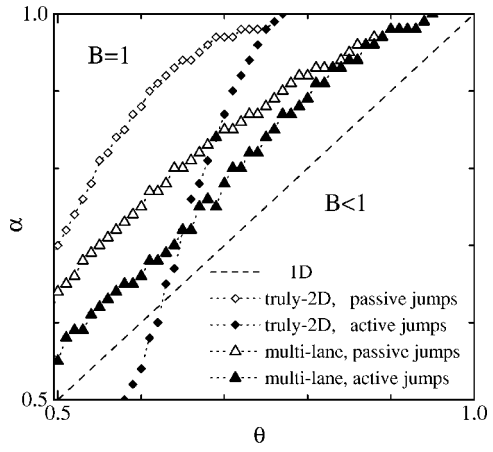

FIG. 12. Phase diagram in the (θ,α) plane. The curves separate the regions where $B=1$ (moving phase, above the curves) and $B<1$ (jamming phase, below the curves). Lattice size is 256×256, and simulation time is 10^5 MC steps per atom.

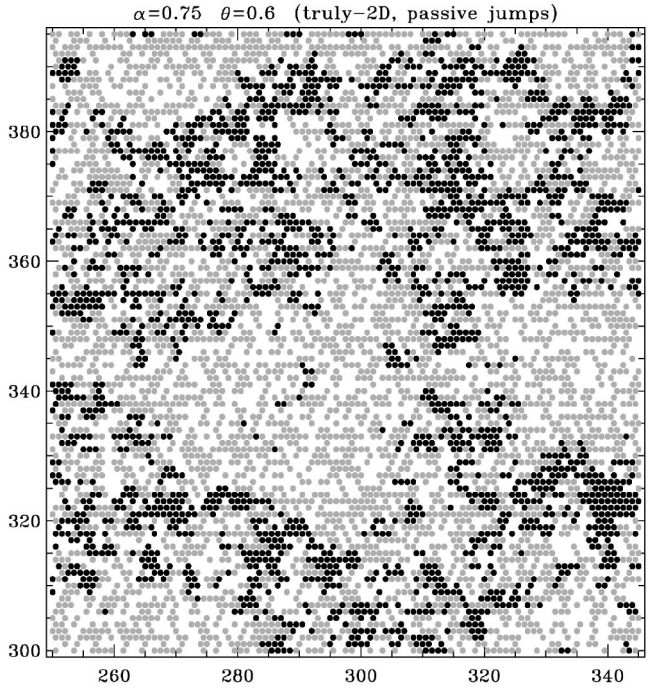

FIG. 13. Snapshot configuration of the truly 2D model with passive jumps for $\alpha=0.75$ and $\theta=0.6$ ($B\approx0.71$). Immobile atoms are in black and running atoms in grey.

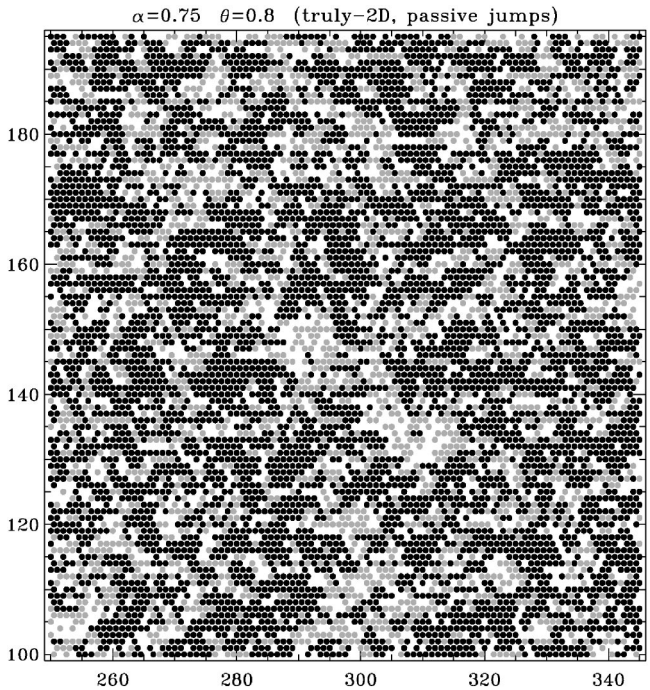

FIG. 14. Snapshot configuration of the truly 2D model with passive jumps for $\alpha=0.75$ and $\theta=0.8$ ($B\approx0.27$). Immobile atoms are in black and running atoms in grey.

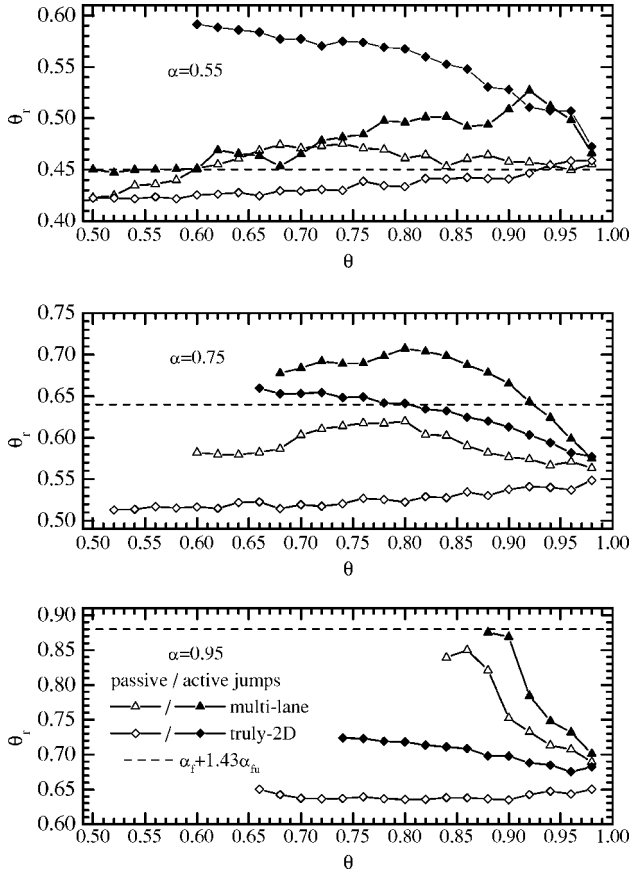

FIG. 15. θ_r vs θ for three values of α (α=0.55, 0.75, and 0.95) extracted from the simulation data with the help of Eq. (2). Triangles are for the multilane model; diamonds are for the truly 2D model; open symbols are for the models with passive jumps and solid symbols for the models with active jumps. The value of $\overline{\alpha}$ is shown by a dashed line.

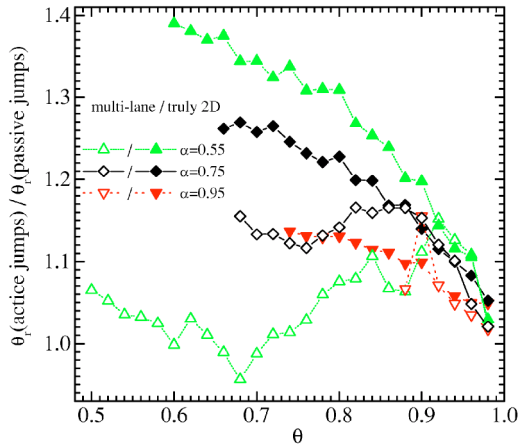

FIG. 16. The ratio of the concentration θ_r for the model with active jumps to that with passive jumps as a function of θ for three values of α (α=0.55, 0.75, and 0.95). Open symbols are for the multilane model and solid symbols for the truly 2D model.

The value θ_r determined above just defines the critical value θ_c which separates the running and jamming states in the phase diagram of Fig. 12. Above this concentration, $\theta > \theta_c$, we may write $N_s \approx (\theta - \theta_c)M \approx 2s_m$. In this approach, however, the value of θ_r does not depend on θ while the simulation results of Fig. 15 show a slow increase of θ_r with θ in the region $\theta_c < \theta < \theta_p$. To explain this effect, one may suppose that $\theta_r = \overline{\alpha}(s_m)Q(s_m)$, where $\overline{\alpha}(s_m)$ decreases but $Q(s_m)$ increases when θ grows, and the latter effect dominates. Besides, we also have to take into account the fact that since immobile islands are not compact, there are small subislands of running atoms inside the immobile islands as can be seen, e.g., in the configuration of Fig. 13. The concentration θ_r in these subislands is larger than that in the "main sea" of running atoms. Thus the average value $\langle \theta_r \rangle$ is larger than θ_r in the "sea," and $\langle \theta_r \rangle$ should increase with θ due to the growing of immobile islands.

The case of low mobility ($B < 0.5$). As mentioned above, the overlapping of immobile islands begins when $s_m/M = \gamma < 0.5$ (recall $M = M_x M_y$), where the percolation threshold γ depends on the shape of islands in a general case. Above the percolation, the running atoms are organized into isolated islands as can be seen from Fig. 14. At higher concentrations, $\theta > \theta_p$, the value of θ_r begins to decrease as θ increases and, because the average radius of the running islands decreases, $\overline{\alpha}$ has to decrease too. Using the relationships $N_s/M = (\theta - \theta_r)/(1 - \theta_r)$ and $s_m \approx 0.5N_s$, we obtain the result that the threshold value $\theta_p(\alpha)$ is coupled with the concentration of the running atoms θ_r by the relationship $2\gamma = (\theta_p - \theta_r)/(1 - \theta_r)$. If we define the value of θ_p as that when θ_r reaches its maximum, from the simulation data for the multilane model with passive jumps we find that $\gamma \approx 0.25$ at $\alpha = 0.55$ (when the island are *y* shaped), $\gamma \approx 0.2$ at $\alpha = 0.75$ (when the islands are approximately circular), and $\gamma \lesssim 0.1$ at $\alpha = 0.95$ (when the island are *x* elongated). These results look reasonable if we assume that the percolation in the driving direction is important only.

V. CONCLUSION

We have studied numerically and, whenever possible, analytically a two-dimensional two-state lattice-gas model which demonstrates a typical behavior of traffic jams, i.e., the steady state of the system is splitting into domains of immobile atoms (jams) and running atoms. Four variants of the 2D model, namely the multilane and truly 2D models with passive and active atomic jumps, show a similar behavior. Contrary to the 1D variant of the model, the 2D model is characterized by a truly steady state with a power law distribution of jam sizes characterized by a universal exponent 3/2. The phase diagram of the model shows that the mobility of the 2D system is lower than the mobility of the 1D model due to a branching behavior of jams.

The lattice-gas model studied in the present work should describe qualitatively the locked-to-sliding transition in the driven underdamped Frenkel-Kontorova model. Such a transition, according to the results of our study, should proceed through an inhomogeneous steady state, where the system

splits into immobile and running domains. Preliminary results show that this indeed is the case at least for some range of model parameters [24,25,27]. Therefore the results of the present work may find applications in problems of conductivity of 2D systems or behavior of tribology systems as was mentioned in the Introduction. Besides, the model studied in the present work may be used to describe granular flow, e.g., grain, corn, or pills flow on inclined hopper surfaces [28] or in a vertical pipe. Finally, the two-state LG model may be useful in investigation of general aspects of "intelligent transport systems" such as multilane traffic, can and bottle transport systems in factories, baggage flow on conveyor belts, data exchange in computer networks, and even emergency escaping in case of crowds of people.

ACKNOWLEDGMENTS

This research was supported in part by the Hong Kong Research Grants Council (RGC) and the Hong Kong Baptist University Faculty Research Grant (FRG). O.B. was partially supported by the NATO Collaborative Linkage Grant PST.CGL.980044.

APPENDIX

The diffusion equation $\partial P(s,t)/\partial t = \partial^2 P(s,t)/\partial s^2$ with the absorbing boundary condition $P(0,t)=0$ at $s=0$ has the solution

$$P(s,t) = \int_0^\infty a(k)\sin(ks)\exp(-k^2 t)dk,$$

where $a(k)$ is determined by the initial distribution, $a(k) = (2/\pi)\int_0^\infty \sin(ks)P(s,0)ds$. For $t \gg 1$ and $s \gg 1$ this distribution approaches the Gaussian one. For example, for the initial distribution $P(s,0) = s\exp(-s^2)$ which has a maximum at $s \sim 1$, the exact solution of the diffusion equation is

$$P(s,t) = \frac{s\exp[-s^2/(4t+1)]}{(4t+1)^{3/2}}.$$

[1] O. M. Braun and Yu. S. Kivshar, *The Frenkel-Kontorova Model: Concepts, Methods, and Applications* (Springer-Verlag, Berlin, 2004); Phys. Rep. **306**, 1 (1998).
[2] O. M. Braun, B. Hu, A. Filippov, and A. Zeltser, Phys. Rev. E **58**, 1311 (1998); O. Braun and B. Hu, J. Stat. Phys. **92**, 629 (1998).
[3] S. Katz, J. L. Lebowitz, and H. Spohn, J. Stat. Phys. **34**, 497 (1984).
[4] J. Krug, Phys. Rev. Lett. **67**, 1882 (1991).
[5] B. Derrida, E. Domany, and D. Mukamel, J. Stat. Phys. **69**, 667 (1992).
[6] T. M. Liggett, *Stochastic Interacting Systems: Contact, Voter and Exclusion Processes* (Springer, New York, 1999), Vol. 324.
[7] G. M. Schütz, in *Phase Transitions and Critical Phenomena*, edited by C. Domb and J. Lebowitz (Academic, London, 2000), Vol. 19, p. 1251.
[8] *Traffic and Granular Flow*, edited by M. Schreckenberg and D. E. Wolf (Springer, Singapore, 1998).
[9] *Traffic and Granular Flow*, edited by D. Helbing, H. J. Herrmann, and M. Schreckenberg (Springer, New York, 2000).
[10] D. Chowdhury, L. Santen, and A. Schadschneider, Phys. Rep. **329**, 329 (2000).
[11] D. Helbing, Rev. Mod. Phys. **73**, 1067 (2001).
[12] K. Nagel and M. Schreckenberg, J. Phys. I **2**, 2221 (1992).
[13] O. Biham, A. A. Middelton, and D. A. Levine, Phys. Rev. A **46**, R6124 (1992).
[14] M. Schreckenberg, A. Schadschneider, K. Nagel, and N. Ito, Phys. Rev. E **51**, 2939 (1995).
[15] W. Knospe, L. Santen, A. Schadschneider, and M. Schreckenberg, Phys. Rev. E **70**, 016115 (2004).
[16] T. Nagatani, J. Phys. A **26**, L781 (1993); Physica A **202**, 449 (1994).
[17] T. Nagatani, J. Phys. Soc. Jpn. **63**, 52 (1994); J. Phys. A **29**, 6531 (1996).
[18] P. Wagner, K. Nagel, and D. E. Wolf, Physica A **234**, 687 (1997).
[19] D. Chowdhury, D. E. Wolf, and M. Schreckenberg, Physica A **235**, 417 (1997).
[20] W. Knospe, L. Santen, A. Schadschneider, and M. Schreckenberg, Physica A **265**, 614 (1999).
[21] T. Nagatani, Phys. Rev. E **48**, 3290 (1993); **59**, 4857 (1999); Physica A **271**, 200 (1999).
[22] T. Horiguchi and T. Sakakibara, Physica A **252**, 388 (1998).
[23] B. H. Wang, Y. R. Kwong, P. M. Hui, and Bambi Hu, Phys. Rev. E **60**, 149 (1999).
[24] O. M. Braun, T. Dauxois, M. V. Paliy, and M. Peyrard, Phys. Rev. Lett. **78**, 1295 (1997); Phys. Rev. E **55**, 3598 (1997).
[25] M. V. Paliy, O. M. Braun, T. Dauxois, and B. Hu, Phys. Rev. E **56**, 4025 (1997).
[26] A set of histograms for different variants and parameters of the 2D model as well as movies illustrating evolution of the model are available at http://www.iop.kiev.ua/~obraun/lattice.htm
[27] O. M. Braun, B. Hu, and J. Tekić, Phys. Rev. E **71**, 026104 (2005).
[28] Kiwing To, Pik-Yin Lai, and H. K. Pak, Phys. Rev. Lett. **86**, 71 (2001).